Orbit Determination of 1999ML via the Method of Gauss

Team Azi-mousse

Manan Khattar

Alberto Mosconi

Emily Zhang

Summer Science Program

Etscorn Observatory in Socorro, New Mexico

July 23, 2016

Abstract

The near-earth asteroid 1999ML was observed by Manan Khattar, Alberto Mosconi, and Emily Zhang over the course of several weeks with the C-14 telescope at Etscorn Observatory. The images were subsequently processed and analyzed with CCDSoft. Astrometry and photometry were performed on the images, and the resulting data was submitted to the IAU Minor Planet Center. The orbit of the asteroid was determined using the method of Gauss and refined with differential correction and light travel time corrections. Finally, the calculated values were compared to those in the JPL small-body database to check for their accuracy.

Introduction

Our goal was to observe the near-earth asteroid 1999ML, submit our data to the IAU Minor Planet Center, and determine the orbit of the object. In order to achieve this goal, our observation team observed and recorded the position of 1999ML 4 times over the course of several weeks. We ultimately used the data that we collected to determine the orbital elements of this asteroid.

The precise tracking of near-earth asteroids is important because they could potentially pose a threat to Earth. Depending on the size of the asteroid, impact events could cause the loss of many lives or even a mass extinction. Although there is no certain way to prevent such events, it is definitely beneficial to be informed of collisions beforehand so that proper precautions can be taken. In addition, carefully tracking near-earth asteroids would enhance the safety of future spacecrafts and would thus facilitate human space exploration.

Materials and Methods

Our images were taken with the C-14 telescope at Etscorn Observatory. Subsequent reducing, aligning, and combining of the images were performed using CCDSoft. We then used TheSkyX Pro to find stars that allowed us to perform astrometry and photometry on our images. Finally, we wrote our own Python programs that performed the astrometry, photometry, method of Gauss, and corrections.

Our team has had a total of 8 local observations at Etscorn along with 3 remote observation sessions at the Cerro Tololo Inter-American Observatory in La Serena, Chile. At Cerro Tololo, we were clouded out all three times, and therefore did not get any data. Locally, seeing conditions were unfavorable during our first three runs. The seeing conditions for the following three runs, however, were excellent, and we were able to get 3 sets of good data on those nights. Our final two runs were also cloudy, and we collected data for our cloudy night experiments on those two nights. We got our 4th data set when the people who went up for middle shift took photos for all of the asteroids. In addition, we have also taken flat fields, which correct for pixel-to-pixel variations and flaws, that we later shared with the rest of the teams.

During our observing sessions at Etscorn, we always took three sets of 5 visual images of our asteroid along with 11 bias frames and 5 dark frames. The camera chip was always cooled to -5°C. 1999ML is quite bright and very slow moving, so our observing strategy was adapted to meet these conditions. To use its slow speed to our advantage, we took 150 second exposures. On the other hand, to compensate for its slow speed, we tried to wait at least ten minutes between each of our series of five photos. While waiting in between series, we would take our dark frames and bias frames.

In the Method of Gauss, we used the observed right ascension (RA) and declination (Dec) of our asteroid, which we calculated by performing astrometry, to calculate the orbital elements of our asteroid's orbit. First, we stored the right ascension, declination, time of observation, and topocentric Earth-Sun vectors for those times in Python lists. We then calculated the rho-hat vector for each observation, a unit vector pointing in the direction of our asteroid. We then used the recently determined rho-hat vectors and topocentric sun vectors that we got from JPL to put together the scalar equations of range that helped us determine the distances between objects. Next, after finding the Gaussian time intervals, we found the coefficients necessary to solve the the Scalar Equation of

Lagrange, an eighth order polynomial that gives us an initial value for the distance between the Sun and the asteroid. With this initial r value, we calculated the initial values for all three r vectors, or vectors from the Sun to the asteroid, and the rate of change of the r vector for our central observation.

Once these initial vectors were computed, we began our iteration. Alberto and Manan used the truncated Taylor f&g series method, and Emily used the closed form method. The iteration is set up as a while loop that will keep on running until the difference between the old r value and the corrected r value is less than a certain tolerance. Manan and Emily used 10^{-8}, and Alberto used 10^{-9} for this tolerance. In the iteration, for the closed, we first found the change in eccentric anomaly (Delta E) for the first and third observation by using the Newton-Raphson method .With these two Delta E values, we obtained new f and g values, which we used to recalculate our state vectors that we began the loop with. If these corrected state vectors differed largely from the state vectors that we began the iteration with, then the loop continued running.
For the Taylor series we just calculate the truncated fs and gs and update the necessary coefficients to find the new r2dot vector.
In both cases in the iteration we correct for the light travel time, finding where the asteroid really is instead of where we saw it.

Once the old and the corrected state vectors for a certain iteration had a difference that is less than the tolerance, the loop returned our final r and r dot vectors. Finally, we found our orbital elements once we have those vectors.

To find the uncertainties of our orbital elements, we used the Jackknife Method. We wrote a Python program that used resampling to find the uncertainties in the position and velocity vectors of the middle observation. We then added and subtracted these uncertainties from our calculated position and velocity vectors so that we had two new sets of velocity and position vectors for our middle observation, one that is higher than the original and one that is lower than the original. We then ran these two new sets of vectors through our program that determined the orbital elements. Thus, we found a range for each orbital element. Another auxiliary code that we wrote with Python is the SNR Code that calculated the signal-to-noise ratio for each of our observations. Finally, we also wrote a short differential photometry Python program that allowed us to calculate the sky brightness for the 5 nights that we got data.

Attached is an orbit visualization image. In yellow is the orbit and body of our asteroid, 1999ML; the white is the Earth, with the moon orbiting around it. For reference, we included Mars (red) and Venus (pink). In the upper left hand image, we can see that the asteroid passes very close to the orbit of the moon and Earth. In the bottom-most image, we can see that the orbital plane of our asteroid is very close to that of Earth; this will later be shown empirically, as our calculated inclination angle is, in fact, very small. From the upper right hand image, we can see that, at a certain given moment, our asteroid is closer to Earth than either Mars or Venus, thus making it a near-earth asteroid.

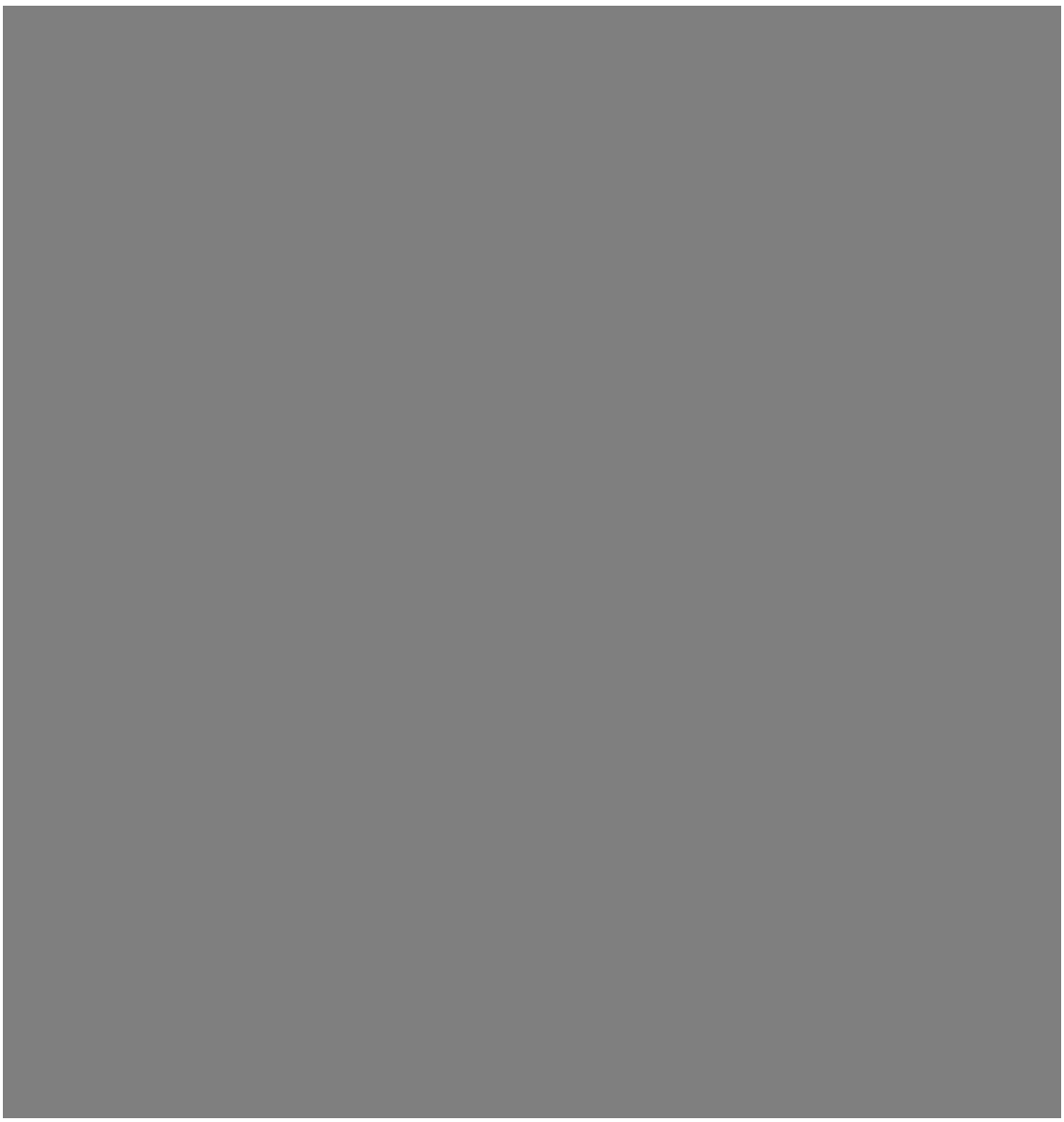

Data and Analysis

We have 4 sets of good data. The table below summarizes our local observations.

Date/Time	Observing Conditions and Sky Brightness	Calculated RA, Dec with Uncertainty	Visual Apparent Magnitude	SNR
6/23/16 7:00-9:00 UTC	Clouded out	N/A	N/A	N/A
6/27/16 5:00-7:00 UTC	Didn't open shutter because of rain	N/A	N/A	N/A
7/1/2016 7:00-9:00 UTC	Clouded out; started cloudy night experiments	N/A	N/A	N/A
7/4/2016 5:00-7:00 UTC	Clear, dark skies; got good data Sky brightness: 25.3863230419	RA: 18:41:52.6754938753 ± 00:00:03.67377009271 Dec: -13:-14:-38.6242156903 ± 00:00:15.4281970148	Mag = 16.356	25.6854220839
7/8/2016 7:00-9:00 UTC	Clear, dark skies; got good data Sky brightness: 24.635902272	RA: 18:42:22.69 ± 00:00:00.327780741196 Dec: -12:44:31.8 ± 00:00:00.447712342369	Mag = 16.281	21.4128932107
7/10/2016	Slightly cloudy, but not in	RA = 18:42:43.31 ±	Mag = 16.280	26.9949705

5:00-7:00 UTC	direction of asteroid Sky brightness: 31.38	00:00:00.0217135606805 Dec = -12:31:19.4 ± 00:00:00.228187209553		009
7/13/2016 7:00-9:00 UTC	Clear, dark skies; got good data Sky brightness: 25.1754398413	RA: 18:43:24.88 ± 00:00:00.271410708046 Dec: -12:11:1.2 ± 00:00:00.396434793365	Mag = 16.257	27.3275164733
7/17/2016 3:00-5:00 UTC	Clouded out; continued cloudy night experiments	N/A	N/A	N/A
7/20/2016 7:00-9:00 UTC	Cloudy; finished cloudy night data collection	N/A	N/A	N/A
7/21/2016 5:00-7:00 UTC Note: the images from this shift were taken by the people who went up for middle shift	Sky was quite bright, so that probably explains the low signal to noise ratio. However, the images are still usable. Sky brightness: 24.157935139	RA: 18:46:37.9760746011 ± 00:00:10.931270992 Dec: -11:-27:-30.9430892529 ± 00:00:07.36010743869	Mag = 16.233	14.3744900933

Acknowledgements to Team 2 (Daniel Michael, Kathryn Chan, and Annie Chen) for providing us with the data from the July 10, 2016 observation.

After the raw images were taken at Etscorn, we reduced, aligned, and combined them with CCDSoft. We then performed astrometry on them to determine their right ascensions and declinations. These values were what we plugged into the method of Gauss to determine the orbit of the asteroid.

To check the validity of our raw data, we compared the images that we took to TheSkyX and made sure that the stars matched up. To check the validity of the values that we calculated for right ascension and declination, we checked our values with those of JPL. In general, our values were well within the calculated uncertainty from JPL's values.

Table containing the orbital elements and uncertainty calculated by each member:

	Semi-major axis (AU)	Eccentricity (no units)	Inclination (degrees)	Argument of periapsis (degrees)	Longitude of ascending node (degrees)	Mean anomaly (degrees)
Brief Description	Determines the size of the orbit; specifies the size of the semi-major axis	Determines the shape of the orbit; specifies how much the elliptic orbit is elongated	Determines the tilt of the orbital plane; the angle between the reference plane and the orbital plane	Determines the twist of the orbital plane; the angle between the ascending node and the vernal equinox	Orients the orbit within the orbital plane; the angle between the ascending node and the periapsis	Places the object in an exact spot on the orbit; angle between the periapsis and the object's position
Manan	2.2676255155to 2.2799331559	0.4553327985 to 0.4565366259	2.746791693 to 2.299642395	112.00223172 to 111.82145886	210.53136697 to 211.65151647	347.0908306 to 346.4371789
Emily	2.2676962183 to 2.2800301557	0.4553455243to 0.4565542427	2.746796116 to 2.299826625	112.00151321 to 111.81862128	210.531710651 to 211.653878048	347.0914411 to 346.4380841
Alberto	2.2676255573 to 2.2799332088	0.4553328093 to 0.4565366349	2.746791530 to 2.299642555	112.00223003 to 111.82145888	210.531366914 to 211.651516113	347.0908317 to 346.4371794

After we calculated our orbital elements, we used them to predict the measured asteroid positions of Team 2. For their observation on July 6, our orbital elements gave us a right ascension and declination that was less than 0.1 seconds and arcseconds away from their measured asteroid position. For their July 10th observation, our orbital elements gave us a right ascension and declination that was accurate up to the millionth decimal place. Finally, for Team 2's July 14th observation, our orbital elements gave us a right ascension that was off by 0.1 seconds and a

declination that was off by 0 .001 arcseconds. In total, our orbital elements predicted the other team's measured asteroid position precisely.

Differential correction did not particularly improve our results. Without it, our predicted right ascension and declination matched the input file values with O-C values in the order of 10e-8 for the central observation and 10e-5 for the first and last observation. With the correction, our orbital elements experienced variations in the third, fourth, or fifth decimal place, making them oscillate within the predicted error bar. It also set off our right ascension and declination values by ≈ 0.01 to 1 arcsecond. In addition,the O-C values did not get smaller after differential correction was applied. This is probably due to the fact that our asteroid is very slow moving. Our predictions have such a close match with the observations that the differential correction is not really effective since just the choice of delta, which can range from 10e-2 to 10e-4 , effectively introduces a bigger uncertainty than the order of magnitude we are trying to correct for.

With or without differential correction, our calculated orbital elements did match up very well with those that are recorded on JPL; the slight differences were well within our uncertainties. Based on our orbital elements, our asteroid is within the asteroid family of Amor.

Conclusion

We are fairly confident in our determined orbital elements as all three of our team members independently calculated orbital elements that were quite close to each other. In addition, our orbital elements match up very well with those on JPL.

Although the entire orbit determination project went, in general, very smoothly for our team, there are a few things that we could have done differently. Firstly, we should have kept up with the right ascension and declination values that we got every time we performed LSPR on data from an observation. Since we did not keep up with these values, we had to rerun our code every time we needed those values. Much time and energy could have been saved by having such foresight from the beginning. Something else that we could have done differently is that we should have encapsulated various codes that we wrote into functions so that they would be easier to call when we needed them. Doing so would make later programming assignments much less daunting.

Despite our attempts to reduce the error in our calculations, certain sources of error are unavoidable. One of the biggest sources of unavoidable error is the noise in our images. This noise comes from a combination of shot noise from both the star and the background and uncertainties in the detection system. In addition, LSPR inherently tries to find the best fit given the reference stars, but due to a lack of the exact positions in the stars and the limitations in our centroid program, the right ascensions and declinations are slightly inaccurate. The method of Gauss is a preliminary orbit determination, as if we used more terms of the Taylor series to find our f & g values, and eliminated other approximations, our position and velocity vectors would have been more accurate. Finally, we

would like to advise a fellow colleague replicating this project to avoid double stars while performing photometry and to be as organized as possible with their programming assignments--having the important functions such as photometry and LSPR encapsulated within convenient functions would have been a lifesaver for us!

Appendices

Appendix A: MPC Report

```
COD 719
CON A. W. Rengstorf
CON [adamwr@pnw.edu]
OBS M. Khattar, A. Mosconi, E. Zhang
MEA M. Khattar, A. Mosconi, E. Zhang
TEL 0.36-m f/11 reflector + CCD
NET NOMAD
BND V
NUM 6
ACK Team 8 - 1999ML

40329         C2016 07 04.23021 18 41 52.88 -13 15 02.1          16.4 V      719
40329         C2016 07 04.25508 18 41 52.80 -13 14 50.9          16.4 V      719
40329         C2016 07 08.31786 18 42 22.67 -12 44 42.6          16.3 V      719
40329         C2016 07 08.36847 18 42 22.67 -12 44 20.6          16.3 V      719
40329         C2016 07 13.31114 18 43 24.78 -12 11 07.2          16.3 V      719
40329         C2016 07 13.35232 18 43 25.07 -12 10 51.2          16.3 V      719
```

Appendix B: Cloudy Night Experiments

Data Collection and Methodology

Our data collection was mostly continuous. After one cloudy day where we were able to get some data but they were either inaccurate or incomplete, on July 17th, we were clouded out once again and so decided to restart data collection. Our data collection proceeded as follows: we first cooled the chip to -5° C, the lowest temperature at which we were supposed to collect data, because it is more energy efficient to cool the chip all at once rather than in regular intervals. We then took a set of biases and temperature-dependent darks at each given temperature. For the temperature-dependent darks, we used a uniform exposure time of 40s. We took most of the temperature-dependent darks that day, and on our next observing shift, we finished the temp.-dependent darks and took the time-dependent ones. For the time-dependent darks, the chip's temperature was at 22°C, 3 degrees less than the ambient temperature, and we took sets of 5 images each ranging from a 5s exposure time to 160s.

Expected Results

For pixel count vs. temperature for the biases, we expect to see no relationship between these two variables; i.e, the temperature does not affect pixel count of the biases. This is because the bias is

simply intended to measure the difference between the pixels and any additional noise added during the process of reading the image from the CCD and converting it into a digital image file. While there is a tiny amount of dark current accumulated during the time the image is read from the CCD, this should ideally be very close to zero. Biases should then theoretically not depend on temperature, and just be an inherent property of the CCD chip. However, because the aforementioned imperfections such as the accumulation of dark current, our data might not have a slope of exactly zero.

For pixel count vs time @ constant temperature for the darks, we expect a linear relationship between exposure time and amount of dark current. Dark current is the current flowing through the CCD chip even when no photons are entering the device, as a result of the random generation of electrons and holes in the depletion region of the device. Logically, the linearly longer the exposure time of the image, the longer time there is for these electronic fluctuations to occur and consequently, the larger the dark current will be.

For pixel count/sec vs. temperature for the darks, we predict some form of exponential decay of signal as temperature increases. This is because we know the dark current is strongly temperature-dependent, and many temperature-dependent processes follow some form of Arrhenius' Law, which entails this form of exponential decay. While this might not be a perfect fit, it should closely resemble the actual relationship.

Results and Analysis

Temperature vs Pixel Count for Biases

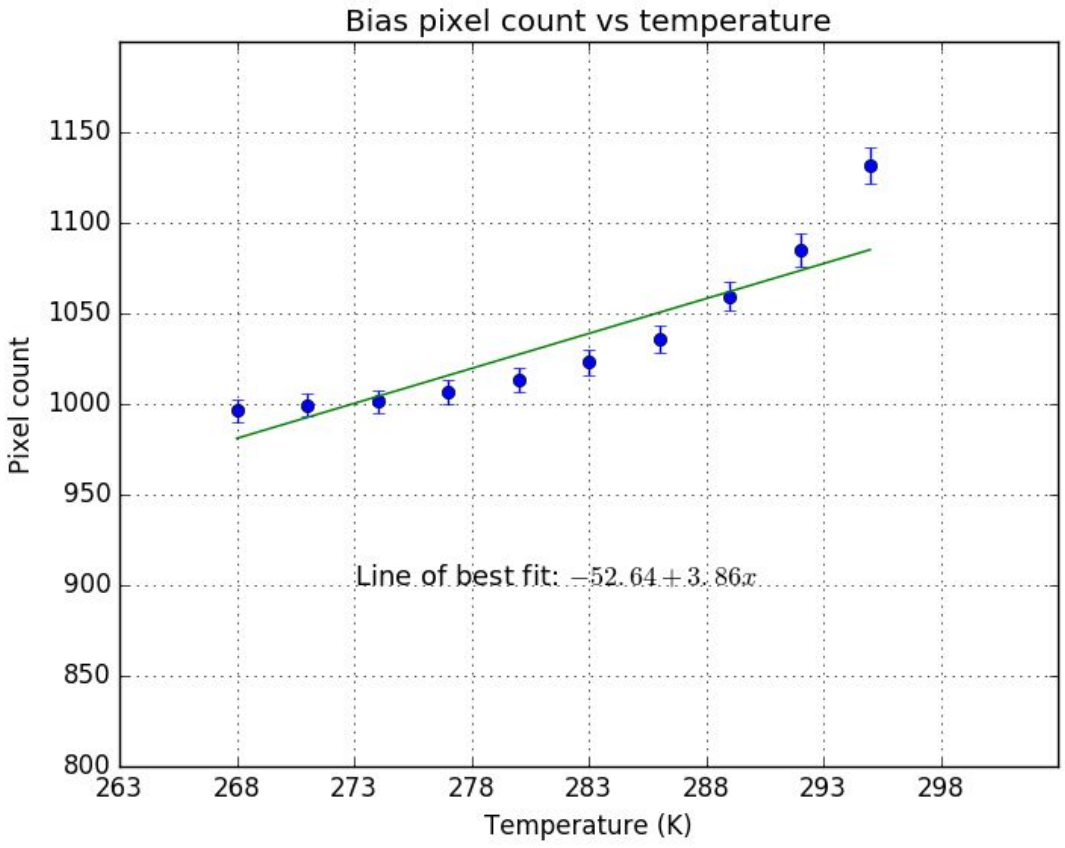

Line of best fit (a + bx): $-52.64 + 3.86x$

$\sigma_a^2 = 6056.487$
$\sigma_b^2 = 0.07775572$
$\sigma_a = 77.823$
$\sigma_b = 0.27885$

Our results did not quite match up with our predictions. We expected the slope to be around zero, because ideally, the pixel value in the biases will not change with changes in temperature. However, the data seem to suggest that the actual relationship of bias with temperature is exponential, albeit slightly so. This could be as a result of the interaction of the dark current with the bias measurement.

Time vs Pixel Count for Darks

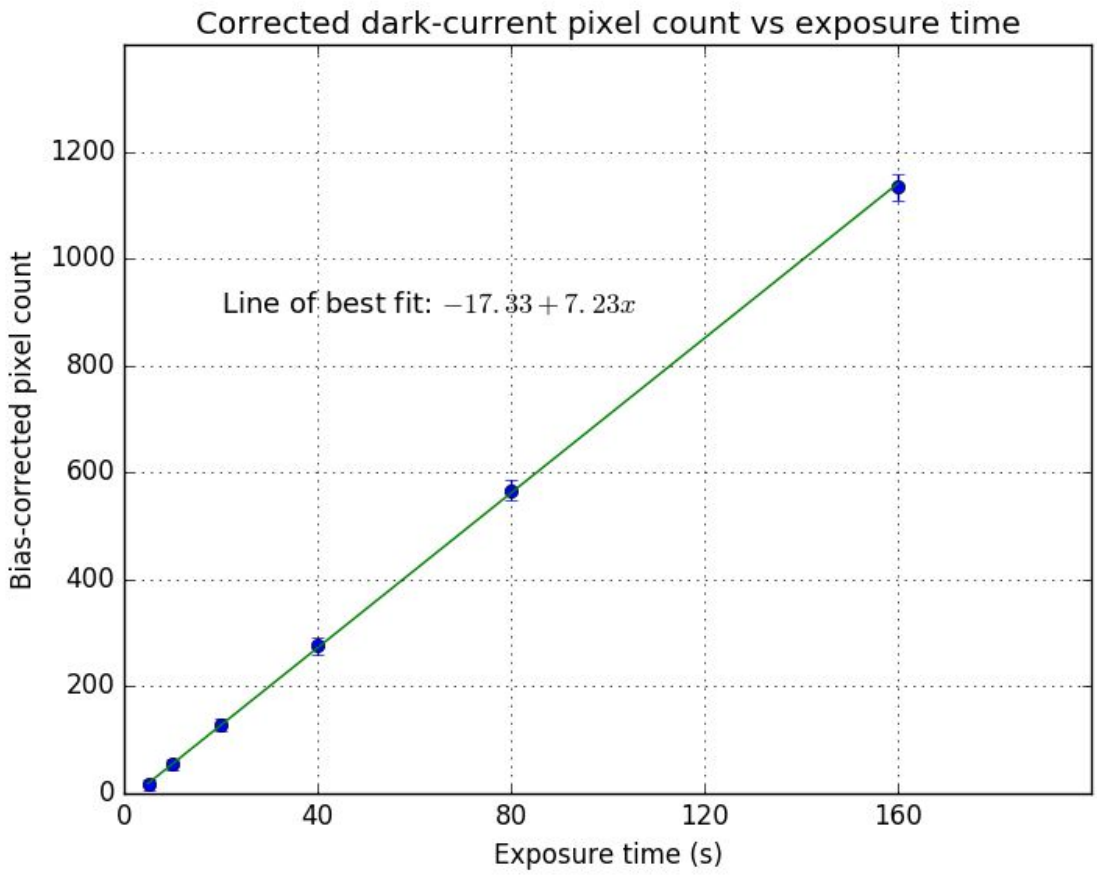

Line of best fit (a + bx): $-17.33 + 7.23x$

$\sigma_a^2 = 48.9489$

$\sigma_b^2 = 0.0224078$

$\sigma_a = 6.996$

$\sigma_a = 0.150$

The time-dependent darks matched our predictions fairly accurately. While we were using ADU as units for the pixel count instead of electrons, as there is a linear relationship between electrons and ADU (the gain), this did not affect the linearity of our data. We also corrected our darks by subtracting the bias count at that given temperature, further bettering the fit of our data. The data seems to be very linear in degree and it is difficult to believe that any fit other than linear would be better for the distribution.

Temperature vs. Pixel Count for Darks

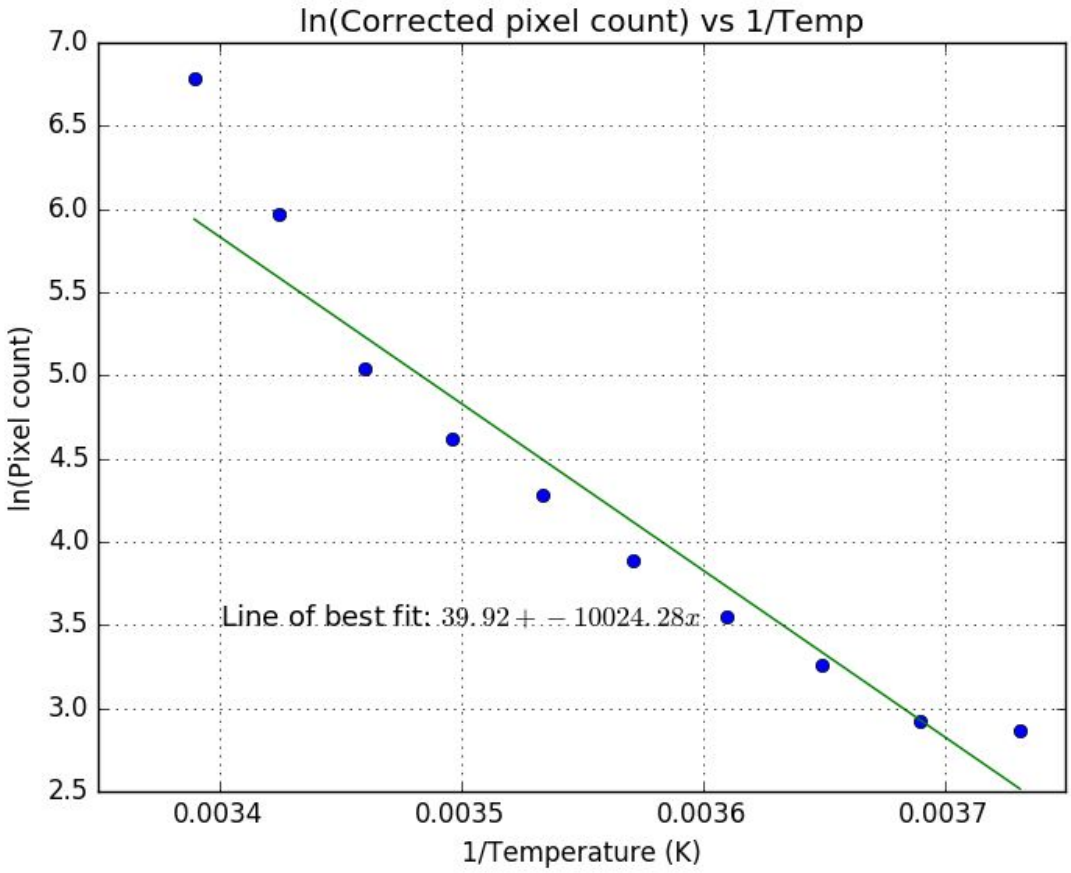

Line of best fit: $39.92 - 10024.28x$

$\sigma_a^2 = 0.00742988$

$\sigma_b^2 = 574.4248$

$\sigma_a = 0.08620$

$\sigma_b = 23.967$

A note: There was a range between -1.9 °C and 2.3 °C when recording data for the -2° C data set, and the 13 °C measurement was taken at 13.2 °C, but this should not produce significant changes in our data. When the y-axis is changed to a log scale and the x-axis becomes the inverse of temperature, the resulting graph looks roughly linear, in accordance with Arrhenius' Law. However, a formulation similar to Arrhenius' Law will require the dark current to be expressed in electrons / second, not ADU/40s, as we have here. The following is the conversion:

$$1\frac{e^-}{s} = 40s \times 10\frac{e^-}{ADU} \times 1\frac{ADU}{40s}$$

When the logarithm of this expression is taken, the result is just the dark current in terms of ADU + a certain factor, so it should not affect the slope. Speaking of the slope, the absolute value of the slope, based on Arrhenius' Law should reflect the "activation energy", so to speak, of the chip. The slope came out to be -10024.28, so the activation energy of the system is 10024.28, with units such that k (the ideal gas constant in Arrhenius' equation) comes out to be 1.

Assuming k to be 1, the pre-exponentiation factor can be calculated in the following way:

$$De^- = De_0^- \times e^{-\Delta E/kT}$$

$$De_0^- = \frac{e^{-\Delta E/kT}}{De^-}$$

At a certain value in the line of best fit, the x-coordinate = 1/Temp = 0.00353, and the y-coordinate is 4.5 = ln(Pixel Count). We know that

$$\ln \frac{e^-}{s} = \ln 4 + \ln \frac{ADU}{40s}$$

So:

$$\ln \frac{e^-}{s} = \ln 4 + 4.5 = 5.8863$$

$$\frac{e^-}{s} = e^{5.8863} = 360.069$$

We now have enough information to plug back into our equation $De_0^- = \frac{e^{-\Delta E/kT}}{De^-}$.

$$De_0^- = \frac{e^{-10024.28 \times 0.00353}}{360.069} = 1.19 \times 10^-18$$

While the above calculation may not be exactly right because of the imprecision of the linear fit, overall it should provide a guideline for if the pre-exponentiation factor is needed to be calculated more accurately.

Conclusion

Overall, these experiments about the various kinds of images used to calibrate and reduce the actual images of our asteroids were mostly enlightening. The bias pixel counts, predicted to not depend on temperature, had a slight exponential growth as temperature increased. This is most likely a result of the small dark current introduced in the CCD chip as it fleetingly records data. The time-dependent darks showed a mostly accurate linear relationship between exposure time and pixel count. The temperature-dependent dark series showed a fairly close linear relationship when plotted with ln(Pixel Count) vs 1/Temp. We then used a modification of Arrhenius' law to estimate what the "activation energy" and pre-exponentiation factor for the model would be, given a certain temperature.

We believe that our initial assumptions were justified, as we based them off of physical approximations and knowledge of the definitions of each type of image. However, being assumptions, they definitely did not take into account all of the factors that go into determining the signal for each image, and we can thus change our assumptions (the dark current introduced as a result of the bias measurement is zero, Arrhenius' Law can be used to model the relationship between temperature and dark current, etc.) based on our results.

Sources:

https://ssp2016nmt.wordpress.com/

http://ssd.jpl.nasa.gov/horizons.cgi

https://www.overleaf.com/read/ywydpqpzxhnk